

Motion stability estimation for modular traction vehicle-based combined unit

V. Bulgakov¹, I. Holovach¹, V. Nadykto², O. Parakhin², H. Kaletnik³,
L. Shymko¹ and J. Olt^{4,*}

¹National University of Life and Environmental Sciences of Ukraine, Ukraine, 15 Heroyiv Oborony Str., UA 03041 Kyiv, Ukraine

²Dmytro Motornyi Tavria State Agrotechnological University, 18B, Khmelnytsky Ave, UA 72310, Melitopol, Zaporozhye Region, Ukraine

³Vinnitsia National Agrarian University of Ukraine, 3 Soniachna Str., UA 21008 Vinnitsia, Ukraine

⁴Estonian University of Life Sciences, Institute of Technology, 56 Kreutzwaldi Str., EE 51006 Tartu, Estonia

*Correspondence: jyri.olt@emu.ee

Abstract. One of the promising ways of efficiently applying high power intensity tractors is their design and utilisation in the form of modular traction vehicles comprising two modules: the power module and the process module. In order to provide for the sufficient manoeuvrability of the modular traction vehicle, when its process module passes a turn, the latter is equipped with vertical and horizontal hinge joints. The freedom of the process module's rotation with respect to the power module in the horizontal plane through the agency of the above-mentioned vertical hinge joint is restrained by a hydraulic cylinder, in which the chambers above and below the piston are connected via a throttle valve with a hydraulic resistance coefficient of about $1.03 \times 10^6 \text{ N m s rad}^{-1}$. This paper is concerned with the theoretical and experimental research into the stability of motion (on turn spaces as well as in the transport mode) of a modular combined unit, when its velocity changes and/or the slip resistance coefficient of the tyres on the wheels of the process module, in which the hydraulic cylinder is equipped with a throttle valve with the above-mentioned hydraulic resistance coefficient, changes.

Key words: modular unit, oscillation, resistance, stability of motion, tractor.

INTRODUCTION

Increasing the power rating of the tractor's engine is one of the ways to improve the productive capacity of combined tractor-implement units. However, the greater the power rating is, the more problematic its utilisation through the agency of the traction effort becomes (Macmillan, 2002). The problem stands out most acutely with tractors in the power intensity category of over 15 kW t^{-1} (Kutkov, 2004).

One of the promising ways of efficiently employing the tractors with high power intensity is their design in the form of modular traction vehicles (Bulgakov et al., 2015, 2019, 2020). With this approach, the traction vehicle comprises two modules: the power

(PM) and the process (PrM) ones (Fig. 1). A wheeled tractor equipped with a ground-speed power take-off shaft is used as the power module. The process module is an additional axle, the wheels of which are driven by the ground-speed power take-off shaft of the power module, that is, the wheeled tractor.

In order to provide for the sufficient manoeuvrability of the modular traction vehicle, when it passes a turn (on turn spaces or during travel runs), its process module is equipped with vertical and horizontal hinge joints. The vertical hinge joint facilitates the angular displacement of the process module relative to the power module in the horizontal plane through angles of $\pm 30^\circ$, while the horizontal hinge joint - through angles of $\pm 15^\circ$ in the transverse and vertical plane.

The details of the design of the connection between the power module and the process module are presented in Fig. 2.

Thus, the ability of the process module to turn relative to power module in the horizontal plane through the agency of the above-mentioned vertical hinge joint 2 is restrained by the hydraulic cylinder 1, in which the chambers above and under the piston are connected through a hose line (Fig. 2).

Besides that, when the modular traction vehicle travels from one field to another one, the process module together with the implement linkage-mounted on it can perform forced oscillations relative to the power module. In many cases, their amplitude is so great that it results in the reduced stability of motion of the process module in the horizontal plane. Eventually, that implies reducing the rate of travel of the whole combined unit, which is an undesirable development.

The issue of research into the stability of motion of articulated power units is extensively covered in the literature (Hac et al., 2008; Szakács, 2010; Yildiz, 2010; Demšar et al., 2012; Song et al., 2014; Pascuzzi, 2015; Li et al., 2016; Nadykto et al., 2019).

However, the earlier obtained results of research are not quite suitable for eliminating the problem under consideration. First of all, it has to be noted that the line of our research is defined by the scientific hypothesis, the essence of which is stated as follows: ‘The stability of motion in the travelling mode of a modular traction vehicle-based combined unit can be improved by means of damping the horizontal oscillations



Figure 1. Modular traction vehicle: PM – power module; PrM – process module.

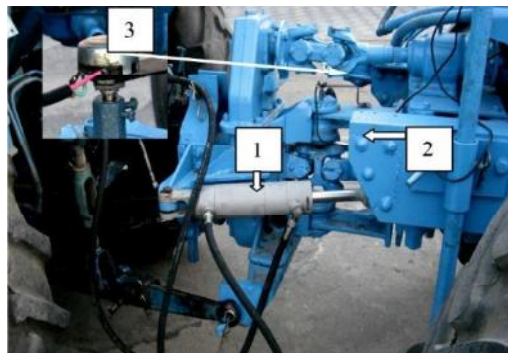


Figure 2. Connection between power and process modules in longitudinal and vertical plane: 1 – hydraulic cylinder; 2 – vertical hinge joint of process module; 3 – resistor SP-3A.

of the process module with respect to the power module, introducing for that purpose a hydraulic damper between the modules'. The said hydraulic damper can be implemented in the form of a throttle valve, which is installed on the line connecting the chambers above and under the piston of the hydraulic cylinder 1 (Fig. 2) and has a resistance coefficient of $1.03 \times 10^6 \text{ N m s rad}^{-1}$ (Bulgakov et al., 2019).

The aim of this completed theoretical and experimental research is to determine the stability of motion in the travelling mode of a modular combined unit in case of varying its rate of travel as well as in case of varying the slip resistance coefficients of the tyres on the wheels of the process module, the linkage hydraulic cylinder of which is equipped with a throttle valve with the earlier indicated hydraulic resistance coefficient.

THEORETICAL PREMISES

It is assumed that the modular combined unit together with the YOX plane performs plane-parallel motion at a constant velocity of V_0 (Fig. 3). The practical experience of operating a multitude of different agricultural combined units has proved that the assumption about the invariance of their operating rate of travel is quite correct.

The above-mentioned plane is tied by its OX axis to the vertical hinge joint of the process module, the centreline of which passes through the point π , which is the effective centre of mass of the modular traction vehicle.

In the YOX plane, the modular traction vehicle-based combined unit has the following three degrees of freedom: 1) transverse displacement X_t of the point π ; 2) course angle φ of the power module; 3) angular displacement β of the process module relative to the longitudinal axis of symmetry of the power module.

When the modular traction vehicle-based combined unit is in the transport mode of motion, the single force F_b (Fig. 3) generated by the rear axle of the power module is sufficient for its movement. Apart from the said force, the following inputs are acting on the modular combined unit: 1) rolling resistance forces applied to the front axle of the power module P_{fa} and to the axle of the process module P_{fc} ; 2) lateral forces P_a , P_b and P_c applied at the points A , B and C , respectively; 3) resultant moment M_m and resultant vector R_m of the external perturbing forces. The latter one is represented here with its longitudinal R_v and transverse R_g components.

The slips of the tyres on the front and rear axles of the power module as well as the axle of the process module are represented by the angles δ_a , δ_b and δ_c , respectively.

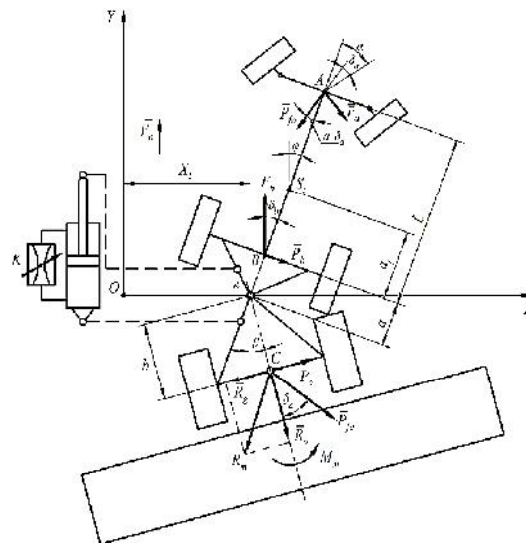


Figure 3. Equivalent schematic model of external forces and moments acting on modular combined unit in horizontal plane.

As mentioned earlier, the mutual angular mobility of the process module and the power module in the horizontal plane is restrained by the hydraulic cylinder, in which the chambers above and under the piston are connected by a throttle valve with a resistance coefficient of K_m .

The mathematical model of the transport mode motion of the modular traction vehicle-based combined unit appears as the system of three differential equations (1). The following designations are used in the system: M_t, J_t – mass of the power module and its moment of inertia about the vertical axis that passes through the point π (Fig. 3); k_a, k_b, k_c – slip resistance coefficients of the tyres on the wheels of the front and rear axles of the power module and the axle of the process module, respectively; J_m – moment of inertia of the process module and the agricultural implement linkage-mounted on it about the axis that passes through the point π ; L, a_m, b_m – design parameters of the modular traction vehicle, which are shown in Fig. 3.

$$\left. \begin{aligned} A_{11} \cdot \ddot{X}_t + A_{12} \cdot \dot{X}_t + A_{13} \cdot \dot{\varphi} + A_{14} \cdot \varphi + A_{15} \cdot \dot{\beta} + A_{16} \cdot \beta &= B_{11} \cdot \alpha - R_g, \\ A_{21} \cdot \ddot{\varphi}_t + A_{22} \cdot \dot{X}_t + A_{23} \cdot \dot{\varphi} + A_{24} \cdot \varphi &= B_{21}, \\ A_{31} \cdot \ddot{\beta}_t + A_{32} \cdot \dot{X}_t + A_{35} \cdot \dot{\beta} + A_{15} \cdot \beta &= M_0, \end{aligned} \right\} \quad (1)$$

The following components are the input variables in the system of differential Eqs (1):

- 1) control action in the form of the angular displacement α of the steer wheels of the power module in the modular traction vehicle;
- 2) perturbing action in the form of the resultant turning moment $M_0 = R_g \cdot b_m - M_m$.

The following components are the output parameters in the functioning of the dynamic system under consideration: displacement X_t of the point π , which is the effective centre of mass of the modular traction vehicle; course angle φ of the power module; angular displacement β of the process module relative to the power module.

The analysis of the stability of motion of the dynamic system under study is best of all performed with the use of the amplitude and phase frequency response characteristics. Currently, these characteristics are efficiently applied for solving similar problems (Yildiz, 2010; Anche & Subramanian, 2018; Ghasemi, 2018). It has been found that just these characteristics represent best of all the stability of a dynamic system in the form of its response to the input perturbing action.

It is to be pointed out that the amplitude frequency response characteristic shows the frequency distribution of the coefficient of the input action amplification by the dynamic system. The phase frequency response characteristic of a dynamic system shows the frequency distribution of the lag in its response to the input action expressed in terms of angle or time values.

In case of follow-up dynamic systems (the system under consideration falls exactly into this category), the ideal amplitude frequency response characteristic and phase frequency response characteristic exist. In particular, the amplification of the input perturbing action by the dynamic system (that is, its amplitude frequency response characteristic) has to be equal to 0 within the whole range of its frequencies (Rotach, 2008). The lag of the dynamic system's response to such an action has to be as great as possible, ideally - tending to infinity (Rotach, 2008).

With such an approach, the mathematical modelling of the stability of motion of a particular dynamic system amounts in essence to selecting such parameters of it, which provide for the best approximation of the ideal amplitude frequency response

characteristic and phase frequency response characteristic by the actual ones.

The actual amplitude frequency response characteristic and phase frequency response characteristic can be obtained from the respective transfer functions. In the case under consideration the transfer function in terms of the turning moment M_0 in relation to the course angle φ of the power module appears as follows:

$$W_1 = \frac{b_6 \cdot p + b_5}{a_6 \cdot p^4 + a_5 \cdot p^3 + a_4 \cdot p^2 + a_3 \cdot p + a_2}. \quad (2)$$

The similar function in terms of the same perturbing action (that is, the moment M_0), but in relation to the angular displacement β of the process module, is more complex:

$$W_2 = \frac{b_4 \cdot p^3 + b_3 \cdot p^2 + b_2 \cdot p + b_1}{a_6 \cdot p^4 + a_5 \cdot p^3 + a_4 \cdot p^2 + a_3 \cdot p + a_2}. \quad (3)$$

The following designations have been assumed in the Eqs (2) and (3):

$$b_6 = A_{15}A_{22},$$

$$b_5 = A_{16}A_{22},$$

$$b_4 = A_{11}A_{21},$$

$$b_3 = A_{12}A_{21} + A_{11}A_{23},$$

$$b_2 = A_{11}A_{24} + A_{12}A_{23} - A_{13}A_{22},$$

$$b_1 = A_{12}A_{24} - A_{22}A_{14},$$

$$a_6 = A_{11}A_{21}A_{31},$$

$$a_5 = A_{12}A_{21}A_{31} + A_{11}A_{31}A_{23} + A_{11}A_{21}A_{35},$$

$$a_4 = A_{11}A_{31}A_{24} + A_{12}A_{23}A_{31} - A_{13}A_{22}A_{31} + A_{11}A_{21}A_{36} + A_{12}A_{21}A_{35} - \\ - A_{21}A_{32}A_{15} + A_{11}A_{23}A_{35},$$

$$a_3 = A_{12}A_{31}A_{24} - A_{22}A_{31}A_{14} + A_{12}A_{21}A_{36} + A_{11}A_{23}A_{36} - A_{21}A_{32}A_{16} + \\ + A_{11}A_{24}A_{35} + A_{12}A_{23}A_{35} - A_{13}A_{22}A_{35} - A_{12}A_{31}A_{24},$$

$$a_2 = A_{11}A_{24}A_{36} + A_{12}A_{23}A_{36} + A_{12}A_{24}A_{35} - A_{13}A_{22}A_{36} - A_{22}A_{14}A_{35} - \\ - A_{23}A_{14}A_{35} - A_{23}A_{32}A_{16} - A_{32}A_{15}A_{24}.$$

The methods and algorithm of calculating the actual amplitude and phase frequency response characteristics of a particular dynamic system, when it responds to both the control and perturbing actions, are in considerable detail described in the book (Rotach, 2008) and many other literary sources. However, before the modelling can be started, it is necessary to verify the adequacy of the developed mathematical model (1). The procedure of this process is described in detail hereafter.

MATERIALS AND METHODS

The adequacy of the mathematical model (1) has been verified by comparing the two amplitude frequency response characteristics. One of them is the theoretical characteristic A_t calculated with the use of the transfer function (3). The second one A_e has been obtained by the authors as a result of their experimental investigation of the combined tractor-implement unit under consideration.

The latter characteristic has been determined in field conditions during the travelling of the modular traction vehicle with a plough mounted on it in the transport mode. The technical specifications of the combined unit under study is presented in Table 1.

Table 1. Technical specifications of modular traction vehicle with plough

Parameter	Designation	Unit	Value
Mass of power module	M_t	kg	3,820
Longitudinal wheel base of tractor	L	m	2.37
Mass of process module	M_m	kg	2,500
Mass of PLN-5-35 plough	M_p	kg	800
Moment of inertia of power module	J_t	kN m s^2	15.7
Moment of inertia of process module with plough	J_m	kN m s^2	15.9
Tyres on front wheels of power module:	9.00R20		
– width	b_a	m	0.24
– diameter	D_a	m	0.95
– air pressure	ρ_a	MPa	0.10
– vertical load on axle	Q_a	kN	12.70
Tyres on rear wheels of power module:	15.5R38		
– width	b_b	m	0.40
– diameter	D_b	m	1.57
– air pressure	ρ_b	MPa	0.12
– vertical load on axle	Q_a	kN	25.30
Tyres on wheels of process module:	16.9R38		
– width	b_c	m	0.43
– diameter	D_c	m	1.69
– air pressure	ρ_c	MPa	0.13
– vertical load on axle	Q_c	kN	32.70
Rolling resistance force by front wheels of power module	P_{fa}	kN	1.27
Tractive effort by rear axle of power module	F_b	kN	10.10
Rolling resistance force by wheels of process module	P_{fc}	kN	3.27
Design parameters shown in Fig. 3	a_m	m	1.22
	b_m	m	1.22
Resistance coefficient of throttle valve on hydraulic cylinder of process module	K_m	N m s rad^{-1}	1.03×10^6

During the experimental investigation, the modular traction vehicle complete with the five-bottom plough mounted on it travelled along the 250 m long record run at a constant speed. The agronomic background, on which the combined tractor-implement unit under consideration performed motion, was a scuffled stubble field of winter wheat. The moisture content of the soil was measured in the layer of 0–10 cm with the use of the MG-44 electronic moisture meter with the following specifications: soil moisture content measurement range - 1–40%; measurement error - $\pm 1\%$; duration of one measurement - below 3 seconds.

The time t_a spent by the combined unit under consideration to cover the 250 m long record run was recorded with the use of the electronic stop watch FS-8200 with a measurement accuracy of up to 0.1 s. Later, the rate of travel V_o of the combined unit under consideration was calculated with the use of the following formula: $V_o = 250 \cdot (t_a)$.

During the experimental investigations, the angular displacement β and the angular acceleration $\ddot{\beta}$ of the modular traction vehicle's process module with a PLN-5-35 five-bottom plough rear-mounted on it were recorded in the PC with the use of an 8-channel analogue-to-digital converter.

The angular displacement β of the process module in the horizontal plane was measured with the use of an SP-3A slide-wire gauge with a straight-line characteristic and a rated resistance of 470 Ohm. The slide-wire gauge was installed on the axle of the vertical hinge joint connecting the power and process modules in the modular traction vehicle (pos. 3, Fig. 2).

The angular acceleration of the process module was recorded with the use of an MMA 7260QT (Freescale Semiconductor) acceleration transducer. Its main specifications were as follows: output signal - analogue; acceleration measurement range - ± 1.5 g; sensibility - 300 mV g^{-1} ; bandwidth - 150 Hz.

In order to use the measurements of the angular displacement β and the angular acceleration $\ddot{\beta}$ obtained as a result of the completed experimental investigations, the standard deviations and the normalized spectral densities have to be calculated with the use of the PC. The obtained statistical characteristics can be used for determining the actual amplitude frequency response characteristic in accordance with the following formula:

$$A_e = \frac{\sigma_\beta}{\sigma_m} \cdot \sqrt{\frac{S_\beta}{S_m}}, \quad (4)$$

where σ_β , σ_m – standard deviations of the oscillations of the angular displacement β of the process module and the turning moment M_o acting on it; S_β , S_m – normalized spectral densities of the oscillations of the angular displacement β of the process module in the modular traction vehicle and the perturbing moment acting on the process module.

The value of the latter is determined with the use of the following expression:

$$M_o = J_m \cdot \ddot{\beta}, \quad (5)$$

where J_m – moment of inertia of the process module complete with the mounted plough about the axis that is aligned with the vertical hinge joint of the process module (point π , Fig. 3). This parameter has been determined by way of calculation.

As already stated above, the experimental amplitude frequency response characteristic has been compared with the theoretical one calculated with the use of the transfer function (3). The parameters present in the said function include the slip resistance coefficients of the tyres on the wheels of the modular traction vehicle k_a , k_b and k_c . Their values depend on the vertical load Q acting on the tyre, its diameter D , width b and air pressure ρ .

In view of the fact that each of the axles of the modular traction vehicle is compliant with the following condition:

$$U = 0.42 \cdot \frac{Q}{\rho \cdot D^2} \cdot \sqrt{\frac{D}{b}} < 0.088, \quad (6)$$

the values of the slip resistance coefficients of their tyres are calculated similarly (Xie, 1984) with the use of the following expression:

$$k = 145(1.7 \cdot U - 12.7 \cdot U^2) \cdot \rho \cdot b^2. \quad (7)$$

The values of the slip resistance coefficients of the tyres k_a , k_b and k_c are calculated by the formula (7) taking into account the data in Table 1. The values obtained as a result are used as one of the analysed parameters in the theoretical calculation of the specially developed mathematical model (1). The reason for choosing the above approach can be explained as follows. Knowing the pattern of the effect the aforesaid coefficients have on the stability of motion of the modules in the modular traction vehicle, it is not difficult to find out with the use of the formula (7) the required values of the air pressure in the tyres on all its wheels. Eventually, that can be efficiently implemented under the practical conditions of operation of the modular traction vehicle.

The second parameter that is variable in the process of theoretical investigations is the rate of travel of the modular traction vehicle-based combined unit in the transport mode. The parameter V_0 varies from 2 to 5 m s⁻¹ (7.2–18.0 km h⁻¹). The smaller speeds of moving in the transport mode are inefficient, while moving at greater rates is restricted by the operating specifications of the modular traction vehicle. These specifications stipulate that the maximum rate of travelling in the transport mode of such a modular vehicle may not exceed 5.5 m s⁻¹.

RESULTS AND DISCUSSION

During the experimental investigations, the soil moisture content of the agronomic background within the layer of 0–10 cm did not exceed 14.5%. The modular traction vehicle with the plough travelled at rates, the mean value of which was equal to 3.95 m s⁻¹. Exactly this value of the motion velocity V_0 was used for calculating the theoretical amplitude frequency response characteristic (A_t) of the investigated tractor-implement combined unit in its response to the perturbing action (moment M_0) with the use of the transfer function (3). The comparison of the obtained characteristic with the experimental one (A_e) has proved their satisfactory convergence (Fig. 4).

Such convergence unequivocally indicates that the mathematical model (1) of the transport mode of travel of a modular traction vehicle with an agricultural implement (in this particular case - a plough) mounted on it is adequate, hence, perfectly suitable for further theoretical investigations.

The further theoretical analysis of the amplitude frequency response characteristic and the phase frequency response characteristic plotted with the use of the transfer function (3) has resulted in the following findings. As the rate of travel of the investigated combined unit rises from 2 to 5 m s⁻¹, the amplitude frequency response

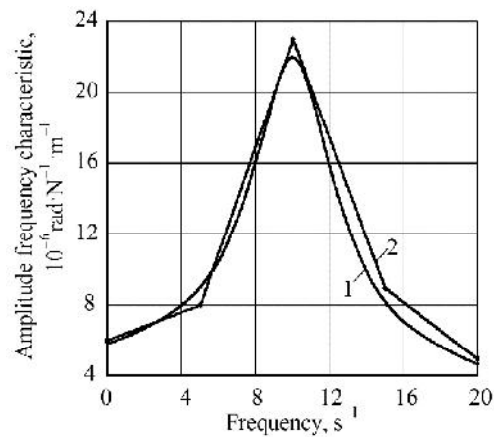


Figure 4. Amplitude frequency response characteristics of investigated combined unit: 1) theoretical A_t ; 2) experimental A_e .

characteristics of the angular displacement β of the process module responding to the perturbing action (moment M_0) reach their resonance peaks at a frequency of 10 s^{-1} (Fig. 5).

At the same time, the amplitude frequency response characteristics themselves change very little, especially at travel rates of $V_0 = 2 \text{ m s}^{-1}$ and higher. That can be explained by the inertia of the process module with the plough mounted on it that becomes more pronounced with the rise of the combined unit's speed.

As regards the phase frequency response characteristics, they vary little within the range of frequencies of $0\text{-}10 \text{ s}^{-1}$ (Fig. 6). A substantial difference in the response lag of the process module responding to the perturbing action occurs at frequencies within the range of $10\text{-}20 \text{ s}^{-1}$, then, again, it disappears.

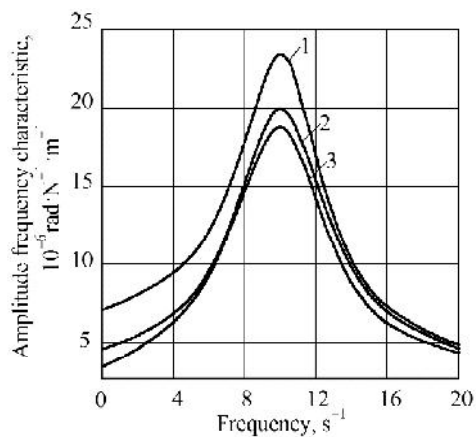


Figure 5. Amplitude frequency response characteristics of angular displacement β of process module responding to perturbing action at different travel rates of modular combined unit (V_0): 1) 2 m s^{-1} ; 2) 3 m s^{-1} ; 3) 5 m s^{-1} .

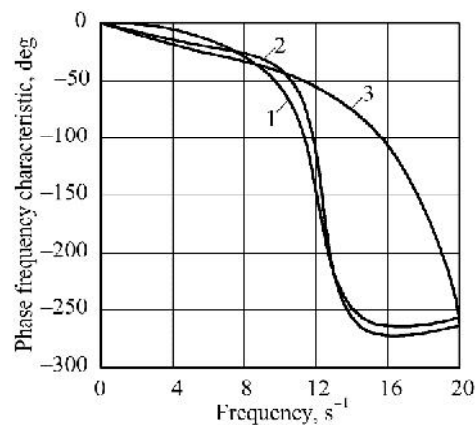


Figure 6. Phase frequency response characteristics of angular displacement β of process module responding to perturbing action at different travel rates of modular combined unit (V_0): 1) 2 m s^{-1} ; 2) 3 m s^{-1} ; 3) 5 m s^{-1} .

It should be reminded that the lag in the response of a dynamic system to a perturbing action has to be as great as possible. In view of that, it is desirable that, when the frequency of oscillations of the angle of the process module is within the range of $10\text{-}20 \text{ s}^{-1}$ ($1.6\text{-}3.2 \text{ Hz}$), the modular combined unit moves at a velocity not exceeding 3 m s^{-1} (Fig. 6). Although, that is applicable more theoretically, than in practice. Here is why.

At a frequency of about 15 s^{-1} the greatest phase difference is observed between the two modes of motion: 2 and 3 m s^{-1} (curves 1 and 2), on the one hand, and 5 m s^{-1} (curve 3), on the other hand. The said difference is specifically equal to about 200° or 3.5 rad . That means that, when V_0 rises from 2 (or 3) m s^{-1} to 5 m s^{-1} , the lag in the response of the process module to the perturbing action decreases by mere $3.5 \cdot 15^{-1} = 0.23 \text{ s}$. At other frequencies within the range of $10\text{-}20 \text{ s}^{-1}$ the difference is even smaller.

That brings to the conclusion that the rate of travelling in the transport mode of the modular combined unit under consideration within its variation range of 2 to 5 m s^{-1} has a negligible effect on the process of oscillation of the angular displacement of the process

module in the modular traction vehicle, when it is under the action of the perturbing action in the form of the turning moment.

Essentially the same can be stated about the slip resistance coefficients of the tyres on the front k_a and rear k_b wheels of the power module.

As regards the slip resistance coefficient k_c of the tyres on the wheels of the process module, the result is different. When its value increases from 160 to 210 kN rad^{-1} , the maximum value of the amplitude frequency response characteristic of the dynamic system rises (curve 2, Fig. 7). The further growth of the value of the coefficient k_c results in the decrease of the said characteristic. At the same time, the resonance peaks of the amplitude frequency response characteristics (curves 3 and 4) shift to the area of higher frequencies.

Although the phase frequency response characteristics differ from each other at frequencies of over 6 s^{-1} , the difference is small (Fig. 8).

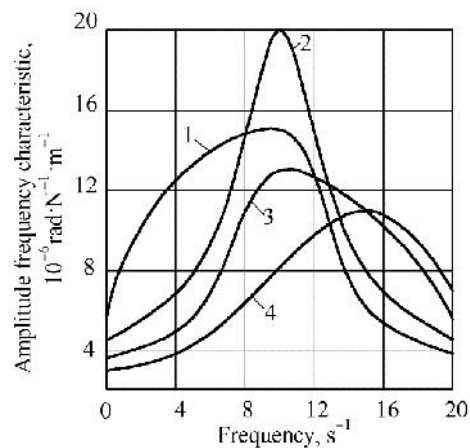


Figure 7. Amplitude frequency response characteristic of angle β of process module responding to perturbing action at different values of coefficient k_c :

- 1) 160 kN rad^{-1} ; 2) 210 kN rad^{-1} ;
- 3) 260 kN rad^{-1} ; 4) 310 kN rad^{-1} .

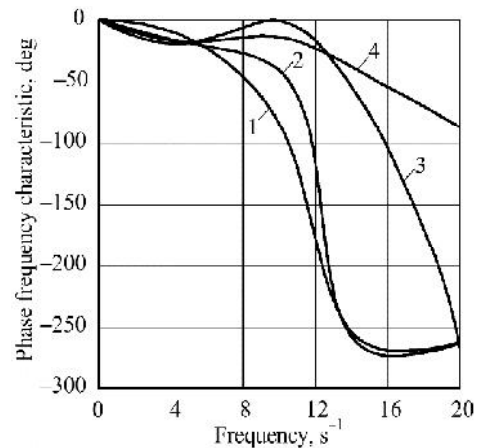


Figure 8. Phase frequency response characteristic of angle β of process module responding to perturbing action at different values of coefficient k_c :

- 1) 160 kN rad^{-1} ; 2) 210 kN rad^{-1} ;
- 3) 260 kN rad^{-1} ; 4) 310 kN rad^{-1} .

The final conclusion is that installing tyres with a slip resistance coefficient of about 260 kN rad^{-1} and higher on the wheels of the process module contributes to the reduction of the amplitude of the module's oscillation in the horizontal plane.

The following step is to analyse the impact that the turning moment M_o has on the dynamics of oscillation of the course angle φ of the power module in the modular traction vehicle. In this case, the amplitude and phase frequency response characteristics are generated with the use of the transfer function (2).

The same as in case of the process module, the variation of the rate, at which the modular combined unit under consideration travels in the transport mode, within the assumed range of $2\text{--}5\text{ m s}^{-1}$ has an insignificant effect on how the power module responds to the perturbing action in the form of the moment M_0 (Fig. 9).

Here, the same as in case of the process module, the resonance peaks of the amplitude frequency response characteristics are found at a frequency of 10 s^{-1} . But the amplitude of oscillations of the angle φ is smaller in comparison to the amplitude of oscillations of the angle β . For example, when the combined unit travels at a rate of 2 m s^{-1} , the maximum value of the amplitude frequency response characteristic of the oscillation of the course angle of the power module (curve 1, Fig. 9) is about 1.9 times smaller than that of the

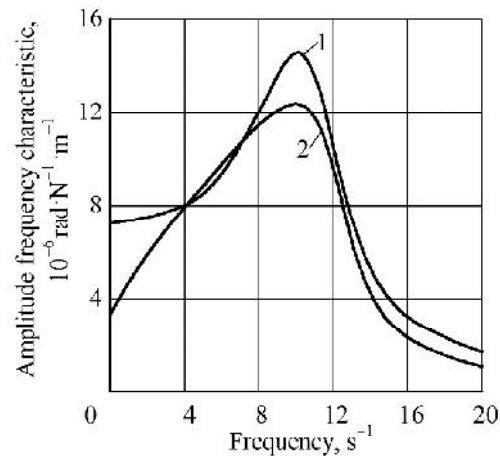


Figure 9. Amplitude frequency response characteristic of angle φ in response to perturbing action at different values of travel rate V_0 : 1) 2 m s^{-1} ; 2) 5 m s^{-1} .

amplitude frequency response characteristic of the oscillation of the angular displacement of the process module (curve 1, Fig. 5). When the rate, at which the modular combined unit travels in the transport mode, is equal to 5 m s^{-1} , the amplitude of oscillations of the angle φ is reduced by factor of 1.5 in comparison to the oscillations of the angle β .

Essentially, such a result is quite logical, since the mass of the power module in the modular combined unit is by 520 kg greater, than the mass of the process module complete with the plough mounted on it. Moreover, the turning moment M_0 acts on the process module with the plough directly, which is not the case for the power module.

The mentioned circumstances are exactly what explains the fact that changing the values of the slip resistance coefficients of the tyres on the wheels of the rear and especially front axles of the power module has little effect on the oscillation of its course angle under the action of the perturbing moment. Theoretically, the value of the discussed coefficient depends mostly on the air pressure in the tyre (Xie, 1984). That implies that in the selection of the value for this parameter (the value of ρ) the preference must be given not to the stability of the power module under the impact of the perturbing action, but to some other factors (for example, the kinematic mismatch between the drives of the axles in the power module).

The dynamics of the lag in the response of the power module to the oscillations of the moment M_0 is as follows. When the perturbing action oscillates at a frequency of under 8.5 s^{-1} , the variation of the travel rate of the combined unit from 2 to 5 m s^{-1} has little effect on the dynamics of the oscillation of the course angle maintained by the power module of the modular traction vehicle (Fig. 10).

Theoretically, within the perturbing moment oscillation frequency range of 8.5–12.5 s⁻¹ it is more advantageous for the modular combined unit to travel at a lower speed, because in that case the lag in the response of the power module to the perturbing action is greater. That is especially true for the perturbing moment oscillation frequencies that are close to 10 s⁻¹ (curve 1, Fig. 10).

At perturbing moment oscillation frequencies of over 12 s⁻¹ it is preferable for the modular combined unit to travel at a greater rate (up to 5 m s⁻¹, curve 2, Fig. 10). When that is complied with, especially at frequencies of over 16 s⁻¹, the desired lag in the response of the power module in the modular traction vehicle to the perturbing action grows by more than 0.5 rad. In terms of time, that is equal to about 0.1 s, which is exactly the expected result.

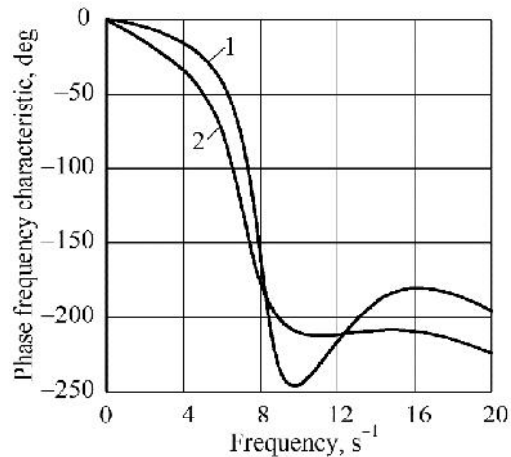


Figure 10. Phase frequency response characteristic of angle φ in response to perturbing action at different values of travel rate V_0 : 1) 2 m s⁻¹; 2) 5 m s⁻¹.

CONCLUSIONS

The mathematical model of the modular traction vehicle-based combined unit moving in the transport mode that has been developed by the authors is adequate. The results of the investigations carried out with the use of this model reveal the following:

1. Changing the rate of travel of the combined unit within the range of 2 to 5 m s⁻¹ does not impair the stability of motion of either the process module or, the more so, the power module in the modular traction vehicle. The characteristics of the modules' amplitude frequency response to the perturbing turning moment improve, although insignificantly, when the parameter V_0 increases. The phase frequency characteristic of the process module in the modular traction vehicle responding to the mentioned moment somewhat deteriorates, but only at relatively high frequencies of its oscillation, that is, at frequencies of more than 10 s⁻¹. The response lag of the power module in the modular traction vehicle is virtually invariable with regard to the changes in the combined unit motion condition within the range of 2–5 m s⁻¹.

2. The values of the slip resistance coefficients of the tyres on the wheels of the power module do not have any noticeable effect on the response of the module to the oscillations of the perturbing moment. At the same time, the value of the slip resistance coefficient of the tyre on each of the wheels of the process module has to be equal to at least 130 kN rad⁻¹.

REFERENCES

- Anche, M. & Subramanian, C., 2018. Model Based Compensator Design for Pitch Plane Stability of a Farm Tractor with Implement. *IFAC-PapersOnLine* **51**, 208–213. <https://doi.org/10.1016/j.ifacol.2018.05.043>
- Bulgakov, V., Kyurchev, V., Nadykto, V. & Olt, J., 2015. Structure Development and Results of Testing a Novel Modular Power Unit. *Agriculture and Agricultural Science Procedia* **7**, 40–44. <https://doi.org/10.1016/j.aaspro.2015.12.028>
- Bulgakov, V., Parakhin, O., Mitkov, V. & Chorna, T., 2019. The Coefficient Determination of a Damper Washer Hydraulic Resistance for Reducing a Technical Module Oscillation Amplitude, in: *Modern Development Paths of Agricultural Production*. Springer International Publishing, Cham, pp. 183–190. https://doi.org/10.1007/978-3-030-14918-5_20
- Bulgakov, V., Kuvachov, V. & Olt, J. 2020. Theory of smoothness of movement of multiple-axle agricultural combined tractor-implement units, *Proceedings of the 31st DAAAM International Symposium*, 10 pp., B. Katalinic (Ed.), Published by DAAAM International, ISSN 1726-9679, Vienna, Austria.
- Demšar, I., Bernik, R. & Duhovnik, J., 2012. A Mathematical Model and Numerical Simulation of the Static Stability of a Tractor. *Agric. Conspec. Sci.* **77**, 143–150.
- Ghasemi, A., 2018. A New Current Controller Design for Tractor Active Suspension Using by Model Order Reduction. *Appl. Sci. Reports* **23–30**. <https://doi.org/10.15192/PSCP.ASR.2018.23.1.2330>
- Hac, A., Fulk, D. & Chen, H., 2008. Stability and Control Considerations of Vehicle-Trailer Combination. *SAE Int. J. Passeng. Cars - Mech. Syst.* **1**, 925–937. <https://doi.org/10.4271/2008-01-1228>
- Kutkov, G.M. 2014. *Tractors and Automobiles: the theory and the technological properties*, Moscow, Kolos, 506 pp. (in Russian).
- Li, Z., Mitsuoka, M., Inoue, E., Okayasu, T., Hirai, Y. & Zhu, Z., 2016. Parameter sensitivity for tractor lateral stability against Phase I overturn on random road surfaces. *Biosyst. Eng.* **150**, 10–23, <https://doi.org/10.1016/j.biosystemseng.2016.07.004>
- Macmillan, R.H., 2002. *The Mechanics of Tractor - Implement Performance*. University of Melbourne, 165 pp. <http://eprints.unimelb.edu.au>.
- Nadykto, V., Karaiev, O., Kyurchev, V. & Beloev, H. 2019. The Efficiency of Tractor Application with Articulated Frame for Cultivating Arable Crops, in: Nadykto, V. (Ed.), *Modern Development Paths of Agricultural Production*. Springer International Publishing, Cham, pp. 161–167. https://doi.org/10.1007/978-3-030-14918-5_17
- Pascuzzi, S. 2015. A multibody approach applied to the study of driver injuries due to a narrow-track wheeled tractor rollover. *J. Agric. Eng.* **46**, 105–114. <https://doi.org/10.4081/jae.2015.466>
- Rotach, V.Y. 2008. *Theory of automatic control*. Moscow Technical University, Power Engineering Institute, 123 pp. (in Russian).
- Song, P., Zong, C. & Tomizuka, M. 2014. A terminal sliding mode based torque distribution control for an individual-wheel-drive vehicle. *J. Zhejiang Univ. Sci. A* **15**, 681–693. <https://doi.org/10.1631/jzus.A1400101>
- Szakács, T., 2010. Developing stability control theories for agricultural transport systems. *Acta Polytechnica Hungarica* **7(2)**, 25–37.
- Xie, L., 1984. *Simulation of tractor-trailer system stability*. SAE Tech. Pap. Iowa State University. <https://doi.org/10.4271/851530>
- Yildiz, S. 2010. *Improving high speed lateral stability of longer and heavier vehicles by active steering*. Master's Thesis, Eindhoven University of Technology, 78 pp., <http://mate.tue.nl/mate/pdfs/12270.pdf>